Supplementary Information

Surface Water Enhances the Uptake and Photoreactivity of Gaseous Catechol on Solid Iron(III) Chloride

Julia Tofan-Lazar and Hind A. Al-Abadleh*

Chemistry Department, Wilfrid Laurier University

Waterloo, ON N2L 3C5 Canada

*Corresponding author email: halabadleh@wlu.ca

Journal: Environmental Science and Technology

Prepared: November 16, 2013

Supplementary Data (13 pages)

1. Experimental Details

Estimating gas phase catechol. The bubbler containing catechol was inserted when needed in the dry air line. The amount of catechol introduced to the DRIFTS chamber was estimated as described earlier in the Supporting Information of reference 1 by bubbling the gas at a flow rate of 202 standard cubic centimeter per minute (sccm) into a KCl solution at pH 3 for a given amount of time followed by measuring its UV-vis absorption at 276 nm. Under these conditions, an absorbance of ca. 0.3 is observed corresponding to a concentration of 0.15 mM of catechol in solution. Using Henry's law constant for catechol at 298 K, which is 4600 mol $kg^{-1}bar^{-1}$ (ref. 2), the gas phase concentration of catechol is estimated to be 32(3) ppb.

Preparing DRIFTS samples. Mechanical mixing of $FeCl_3$ with diamond powder was achieved using a wig-L-bug (no ball) for 1 min or manually till sample becomes completely homogeneous. Efficient and reproducible packing of the sample was obtained using a 4 kg weight for 10 min.

Spectral collection. For the first type of DRIFTS experiments, which were designed to examine the role of light and surface water on the uptake of gas phase catechol on solid $FeCl_3$), eighty spectra were collected in the first 10 min by averaging 10 scans at 8 cm^{-1} resolution. Then, ten spectra were collected for the next 50 min by averaging 100 scans at the same resolution.

Irradiance measurements of the light source. A NIST-calibrated fiber optic radiometer (StellarNet Inc.) was used to measure the irradiance of the solar simulator in the wavelength range (300-800 nm) at the surface of the reaction cup. To estimate light irradiance without saturating the detector, a neutral density filter (2”x2”, FSQ-ND05, Newport Corp.) was added to cut intensity by half. After correcting for this intensity reduction, all DRIFTS experiments were conducted using about 4892 Wm^{-2} in the 300-400 nm spectral range (Figure S1).

2.

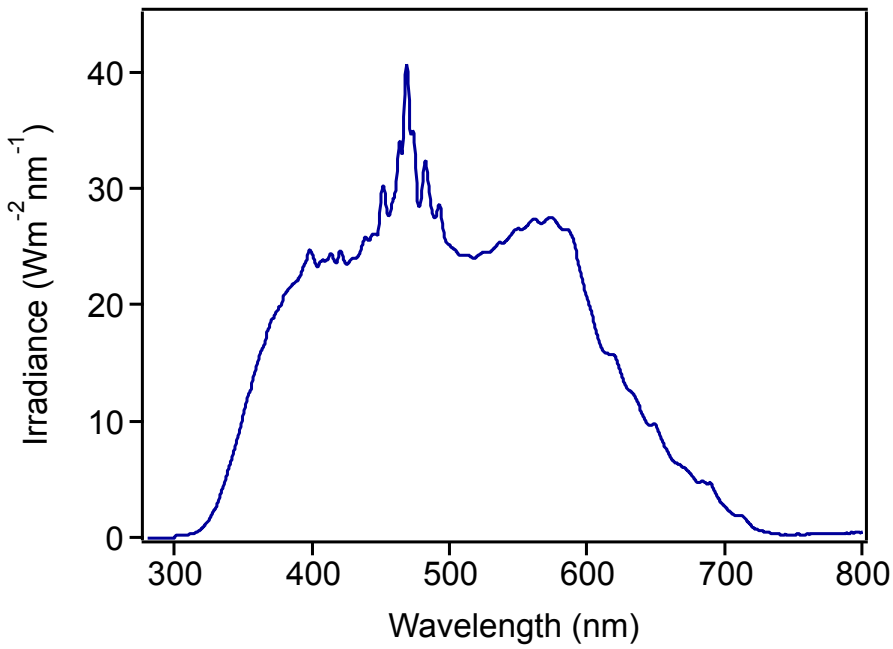

Figure S1: Irradiance spectrum of the solar simulator as measured at the surface of the receptor in place of the reaction chamber after passing through the quartz viewing window.

3.

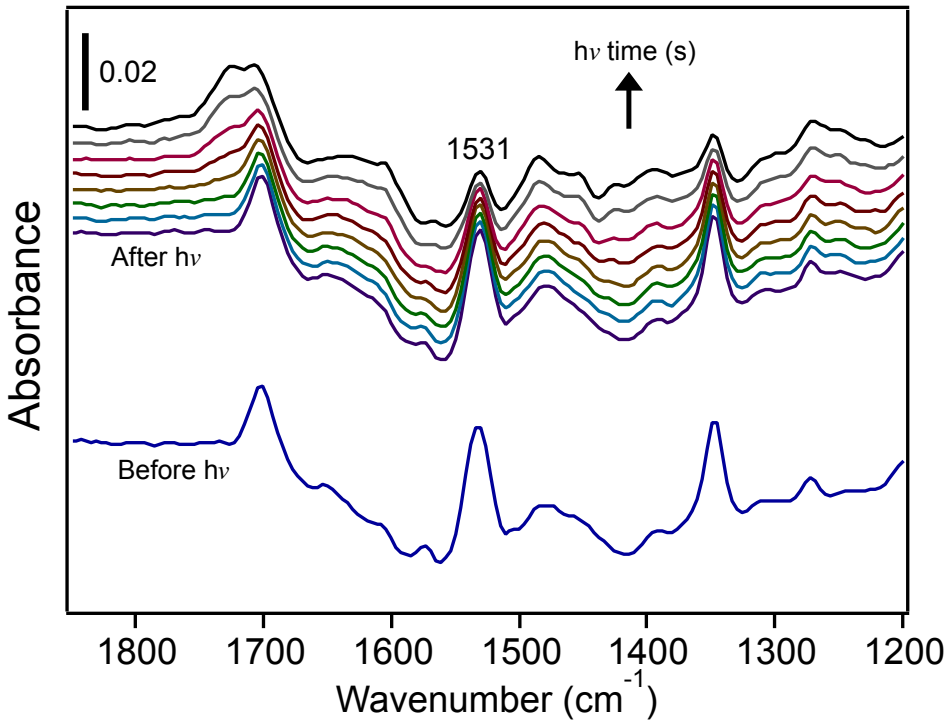

Figure S2: DRIFTS absorbance spectra for the photoisomerization of *o*-nitrobenzaldehyde (2-NB, 0.05% (w/w) in diamond powder) at RH=30%. Spectra were referenced to dry diamond powder sample spectrum. Gas phase water lines between 1500-1700 cm^{-1} were manually subtracted out using a gas phase water only spectrum. Bottom spectrum shows sample before irradiation, and top set of spectra were collected as a function irradiation time (from bottom): 4, 12, 20, 32, 60, 120, 300 and 600 s. The kinetic curve for the decrease in the intensity of the peak at 1531 cm^{-1} is shown in Figure 1(b).

4.

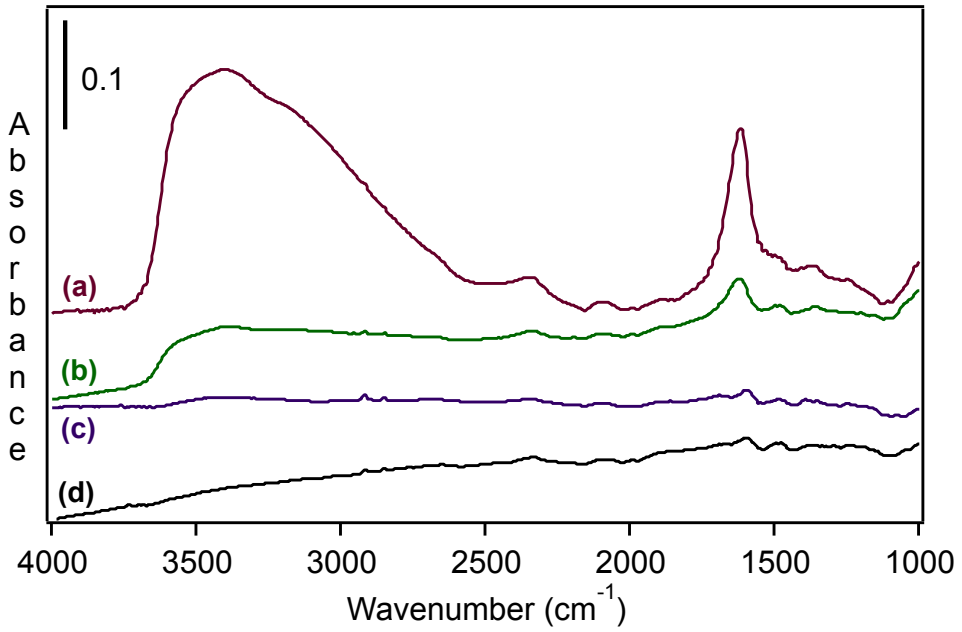

Figure S3: DRIFTS absorbance spectra used as background for referencing spectra collected as a function of catechol uptake in the dark and as a function of irradiation time, under dry and humid conditions, in Figures 2 and 4 of the manuscript. These spectra were referenced to diamond only single beam spectrum: (a) 1%$FeCl_3$ in diamond at 30%RH after 15 min irradiation, prior to introducing catechol vapor, (b) 1%$FeCl_3$ in diamond at 30%RH after 30 min equilibrium in the dark, prior to introducing catechol vapor, (c) 1%$FeCl_3$ in diamond after overnight drying and after 15 min irradiation, prior to introducing catechol vapor, and (d) 1%$FeCl_3$ in diamond after overnight drying in the dark, prior to introducing catechol vapor.

5.

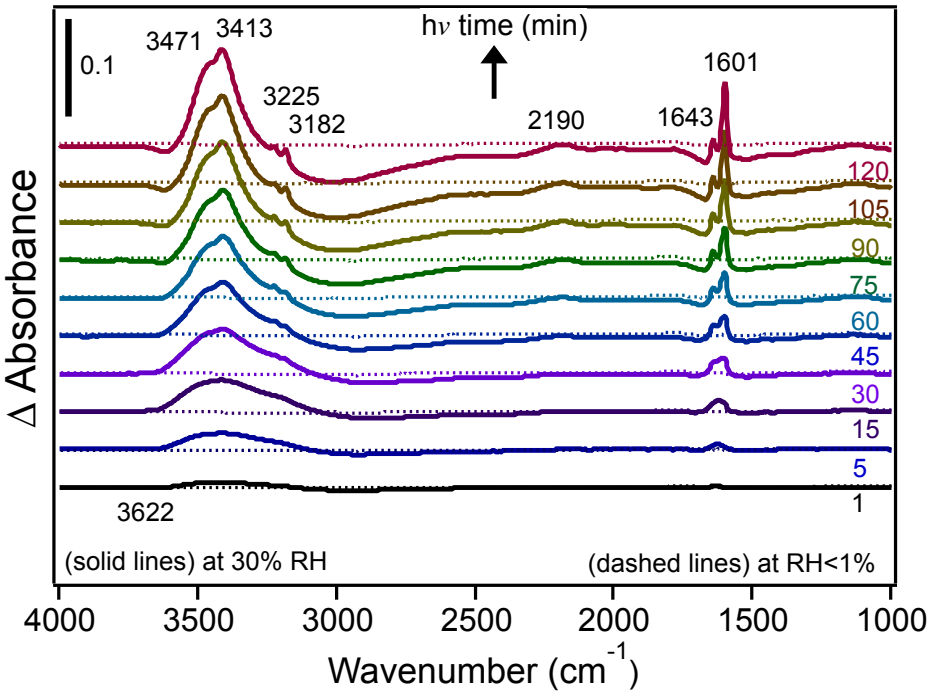

Figure S4: Difference DRIFTS absorbance spectra collected at 30%RH (solid lines) and under dry conditions (dashed lines) as a function of irradiation for a sample containing 1%$FeCl_3$ (w/w) in diamond powder in the absence of adsorbed catechol (as a control experiment).

6. Fitting equation for data in Figure 2(c):

The kinetic curves in Figure 2(c) show the increase in the integrated absorbance from 1558-1018 cm^{-1} assigned to surface catechol in the presence of 1% $FeCl_3(s)$ as a result of flowing gas phase catechol under dry and humid conditions, both in the dark and irradiation. The equation used to fit the data is an empirical sigmoidal growth equation:

$$f(t) = \text{base} + \left\{ \frac{\text{max}}{1 + \exp\left[k \cdot \left(t_{half} - t\right)\right]} \right\} \qquad \text{(Eq S1)}$$

The following table lists the best-fit parameters for the curves shown in Figure 2(c):

Reaction conditions	base	max	k (min^{-1})	t_{half} (min) [a]	Growth factor ($k*t_{half}$)
30%RH, h*ν*	-0.6	6.5	0.077	34	2.6
30%RH, dark	-0.8	10	0.045	55	2.5
RH<1%, h*ν*	-0.3	2.6	0.064	32	2
RH<1%, dark	-0.2	1.6	0.056	33	1.8

Note: [a] represent the time it takes to reaching half the concentration of total surface catechol over the total time of 60 min. Relative growth factor between humid and dry to reaching half catechol surface coverage is about 1.4. Over the 60 min period shown in Figure 2(c), the total relative growth rate is 2(1.4) = 2.8.

7. Estimations of radical formation

At 30%RH, below the deliquescence of $FeCl_3$, water adsorption will result in partial dissolution of this hygroscopic salt, which forms a supersaturated solution of $FeCl_3$. The concentration of this solution equals the maximum solubility of $FeCl_3$ in water at 25°C, 91.2 g/100 g H_2O (5.6 M).[3]

From the bulk speciation of Fe(III) in chloride solutions, the equilibrium constants for the formation of chloro- and hydroxyl- iron species at pH ≤ 3 and 25°C are:[4]

$$[Fe(H_2O)_6]^{3+} \rightleftharpoons [Fe(H_2O)_5(OH)]^{2+} + H^+, \quad K_{eq1} = 6.5\times10^{-3}\ M \qquad \text{(Eq S2)}$$

$$[Fe(H_2O)_6]^{3+} \rightleftharpoons [Fe(H_2O)_4(OH)_2]^{+} + 2H^+, \quad K_{eq2} = 2.1\times10^{-6}\ M^2 \qquad \text{(Eq S3)}$$

$$[Fe(H_2O)_6]^{3+} + Cl^- \rightleftharpoons [Fe(H_2O)_5Cl]^{2+} + H_2O, \quad K_{eq3} = 30.2\ M^{-1} \qquad \text{(Eq S4)}$$

$$[Fe(H_2O)_6]^{3+} + 2Cl^- \rightleftharpoons [Fe(H_2O)_4Cl_2]^{+} + 2H_2O, \quad K_{eq4} = 134.9\ M^{-2} \qquad \text{(Eq S5)}$$

Using Mathematica, the following plot can be generated that shows the fraction of iron species as a function of pH

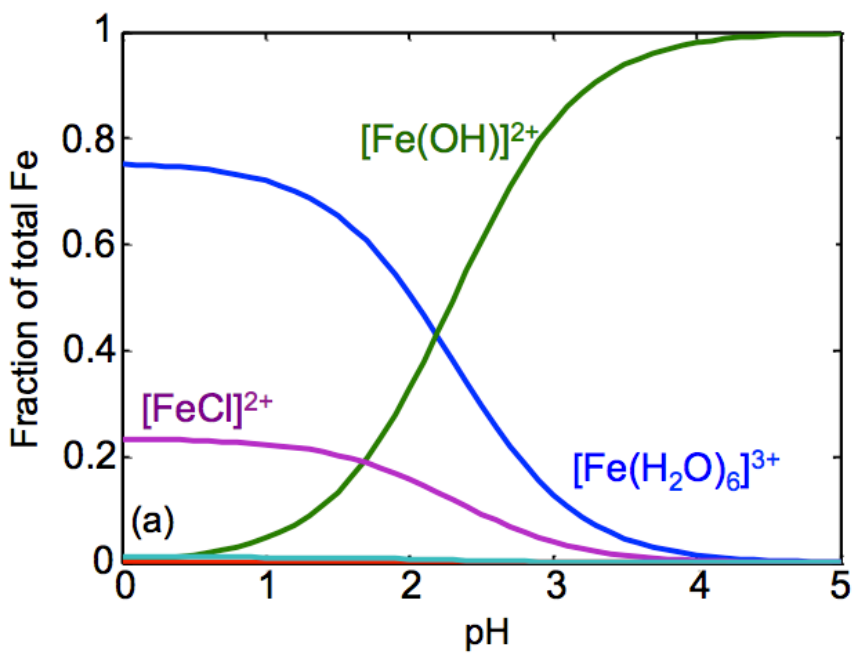

Hence, at pH values below 2 that arise from supersaturated $FeCl_3$ solutions, the concentration of $[Fe(H_2O)_5Cl]^{2+}$ can be calculated to be:

$[Fe(H_2O)_5Cl]^{2+}$ = 0.25 (5.6 M) = 1.4 M

The photolysis of $[Fe(H_2O)_5Cl]^{2+}$ according to equation S6 produces

$$[Fe^{III}(H_2O)_5Cl]^{2+} \xrightarrow{h\nu, H_2O} [Fe^{II}(H_2O)_6]^{2+} + {}^{\bullet}Cl, \quad j_{Cl} \qquad \text{(Eq S6)}$$

where j_{Cl} is the photolysis rate, which equals $2.303 \cdot \varepsilon_{avg} \cdot \Phi \cdot E$, where ε_{avg} is the average molar absorptivity ($M^{-1}cm^{-1}$), Φ is the quantum yield (molecule/photon) and E is the cumulative photon flux from the solar simulator (photons cm^{-2} s^{-1}). The value of ε_{avg} is 875 M^{-1} cm^{-1} (1.45×10^{-18} cm^3 $molecule^{-1}$) in the spectral range 290-405 nm from the UV-vis spectrum of $FeCl_3$(aq) at pH 1 collected in our lab. The value of E in the same spectral range calculated using 2-NB actinometry is detailed in the text and equals $4.9(1)\times10^{15}$ photons cm^{-2} s^{-1}. The value of Φ_{bulk} is 0.5±0.1 molecule/photon as determined from laser kinetic spectroscopy for $[Fe^{III}(H_2O)_5Cl]^{2+}$ in bulk aqueous phase.[5] The value of $\Phi_{interface}$ at the solid/humid air interface is expected to be higher than that in the aqueous phase per calculations done by Nissenson *et al*. on a similar system, $[Fe^{III}(H_2O)_5OH]^{2+}$.[6] Hence, the value of Φ_{bulk} is considered a lower limit for $\Phi_{interface}$. Hence, the value of j_{Cl} is 0.0082 s^{-1} using the light source in our experiment. Scaling this j_{Cl} to the average solar radiant output in the same wavelength range for noontime in Waterloo, Ontario on July 1 is approximately 6×10^{14} photons cm^{-2} s^{-1} [7] will give a value of 0.001 s^{-1}.

The above numbers can be used to estimate the concentration of $[Fe^{III}(H_2O)_5Cl]^{2+}$ and ${}^{\bullet}Cl$ produced as a function of time using first order decay kinetics of $[Fe^{III}(H_2O)_5Cl]^{2+}$ (Eq S7) and first order formation kinetics of ${}^{\bullet}Cl$ (Eq S8), respectively:

$$[Fe^{III}(H_2O)_5Cl]^{2+} = [Fe^{III}(H_2O)_5Cl]_0^{2+} \cdot e^{-j\,t} \qquad \text{(Eq S7)}$$

$$[{}^{\bullet}Cl] = [Fe^{III}(H_2O)_5Cl]_0^{2+} \; (1 - e^{-j\,t}) \qquad \text{(Eq S8)}$$

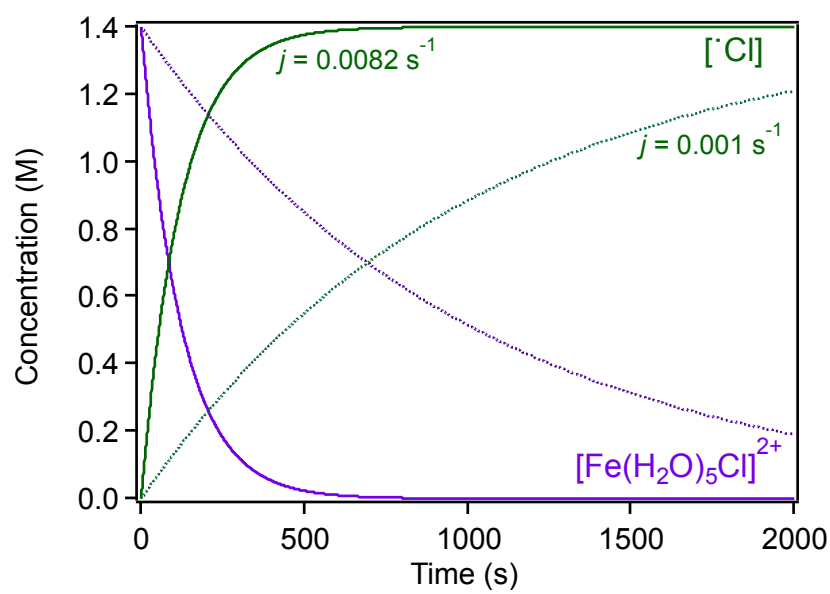

8. Estimations of lifetime of organics from reaction with Cl radicals in the aqueous phase

Reactions of Cl radicals in the bulk aqueous phase are relevant to those occurring in large cloud droplets. It was concluded from a review of these reactions that Cl atoms are formed in cloud droplets as secondary radicals from precursor radicals of higher oxidizing power, such OH during daytime and NO_3 during nighttime, according to these reactions:[8]

$$OH + Cl^- \rightleftharpoons ClOH^- \quad \text{(Eq S8)}$$
$$ClOH^- + H^+ \rightleftharpoons HClOH \quad \text{(Eq S9)}$$
$$HClOH \rightleftharpoons Cl + H_2O \quad \text{(Eq S10)}$$

and

$$NO_3 + Cl^- \rightleftharpoons Cl + NO_3^- \quad \text{(Eq S11)}$$

The average concentration of Cl radicals in the gas phase is 10^4 radicals cm^{-3} (4×10^{-16} atm).[7] Using Henry's law constant for Cl, $K_H = 0.2$ M atm^{-1} at 298 K[9], the concentration of Cl radicals in the aqueous phase is calculated to be 8×10^{-17} M.

In his review on the Kinetics of Aqueous Phase Reactions Relevant for Atmospheric Chemistry[8], Herrmann listed the values of rate constants of Cl radical reactions with organic molecules at room temperature. The highest value is reported for Cl reaction with benzene in the pH range 2.5-3 with $k = 6\times10^9$ $M^{-1}s^{-1}$ at 298 K. Using this value and the above [Cl(aq)], the lifetime of benezene due to reaction with Cl is calculated to be $1/(8\times10^{-17}\,M \times 6\times10^9\,M^{-1}s^{-1}) = 2\times10^6$ s (23 days).

9.

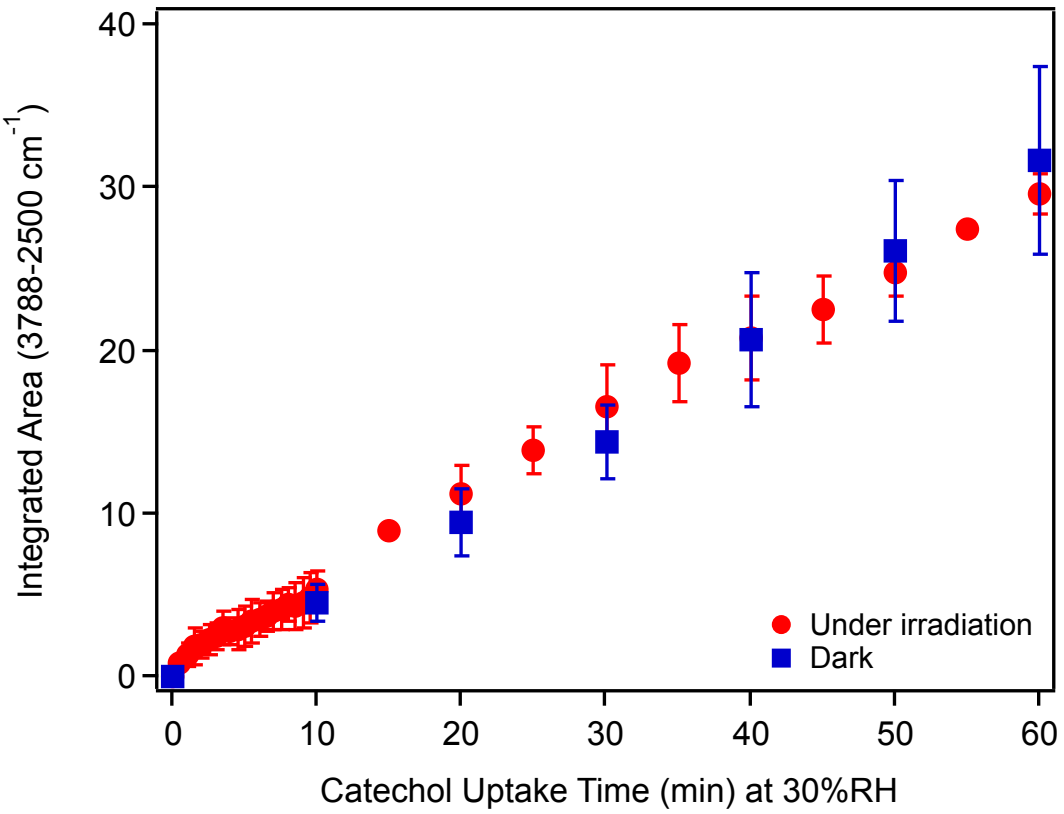

Figure S5: Continuous water uptake on samples containing 1%$FeCl_3$ (w/w) in diamond powder as a function catechol uptake time at 30%RH under irradiation and dark conditions. Some of the spectra used in generating this graph are shown in Figures 4(a) and (b).

10. References:

(1) Tofan-Lazar, J.; Situm, A.; Al-Abadleh, H.A., DRIFTS studies on the role of surface water in stabilizing catechol-iron(III) complexes at the gas/solid interface. *J. Phys. Chem. A* **2013**, *117*, 10368-10380.

(2) *NIST Chemistry WebBook (*http://webbook.nist.gov/chemistry/), Henry's law data for catechol. Accessed January 2013.

(3) Lide, D.R., Ed. *Crc handbook of chemistry and physics*; Taylor & Francis: Boca Raton, 2012-2013; Vol. 93.

(4) Lim, M.; Chiang, K.; Amal, R., Photochemical synthesis of chlorine gas from iron(III) and chloride solution. *J. Photochem. Photobio. A-Chem.* **2006**, *183*, 126-132.

(5) Nadtochenko, V.A.; Kiwi, J., Photolysis of $FeOH^{2+}$ and $FeCl^{2+}$ in aqueous solution. Photodissociation kinetics and quantum yields. *Inorg. Chem.* **1998**, *37*, 5233-5238.

(6) Nissenson, P.; Dabdub, D.; Das, R.; Maurino, V.; Minero, C.; Vione, D., Evidence of the water-cage effect on the photolysis of NO_3^- and $FeOH^{2+}$. Implications of this effect and of H_2O_2 surface accumulation on photochemistry at the airewater interface of atmospheric droplets. *Atmos. Environ.* **2010**, *44*, 4859-4866.

(7) Finlayson-Pitts, B.J.; Pitts Jr., J.N. *Chemistry of the upper and lower atmosphere*; Academic Press: New York, 2000.

(8) Herrmann, H., Kinetics of aqueous phase reactions relevant for atmospheric chemistry. *Chem. Rev.* **2003**, *103*, 4691-4716.

(9) Bräuer, P.; Tilgner, A.; Wolke, R.; Herrmann, H., Mechanism development and modelling of tropospheric multiphase halogen chemistry: The CAPRAM halogen module 2.0 (HM2). *J. Atmos. Chem.* **2013**, *70*, 19-52.